ity to totally inhibit the GAP activity of RGS proteins for their correct cellular targets. Thus, the palmitoylation-depalmitoylation cycle may control both the signal amplitude and the temporal response in G-protein pathways. Palmitoylation can amplify G protein–mediated signals or, alternatively, regulated depalmitoylation could serve as either an off-switch or signal attenuator. Such controls may be G protein–specific, and their complete elucidation awaits better understanding of the control of palmitate addition and removal. Regardless, any of these mechanisms would be compatible with the enhanced binding of palmitoylated Gα to Gβγ (*7*), which would serve to lower background signaling in the absence of stimulation. Regulation of GAP activity may be a major function of Gα palmitoylation.

REFERENCES AND NOTES

1. P. B. Wedegaertner, P. T. Wilson, H. R. Bourne, *J. Biol. Chem.* **270**, 503 (1995); S. M. Mumby, *Curr. Opin. Cell Biol.* **9**, 148 (1997); E. M. Ross, *Curr. Biol.* **5**, 107 (1995); G. Milligan *et al.*, *Biochem. Soc. Trans.* **23**, 583 (1995); C. Kleuss and A. G. Gilman *Proc. Natl. Acad. Sci. U.S.A.* **94**, 6116 (1997).
2. M. E. Linder *et al.*, *Proc. Natl. Acad. Sci. U.S.A.* **90**, 3675 (1993).
3. P. B. Wedegaertner and H. R. Bourne, *Cell* **77**, 1063 (1994).
4. S. M. Mumby, C. Kleuss, A. G. Gilman, *Proc. Natl. Acad. Sci. U.S.A.* **91**, 2800 (1994).
5. D. Stanislaus, J. A. Jovanovick, S. Brothers, P. M. Conn, *Mol. Endocrinol.* **11**, 738 (1997).
6. M. Y. Degtyarev, A. M. Spiegel, T. L. Z. Jones, *J. Biol. Chem.* **268**, 23769 (1993); *ibid.* **269**, 30898 (1994).
7. T. Iiri, P. S. Backlund Jr., T. L. Z. Jones, P. B. Wedegaertner, H. R. Bourne, *Proc. Natl. Acad. Sci. U.S.A.* **93**, 14592 (1996).
8. M. A. Grassie *et al.*, *Biochem. J.* **302**, 913 (1994); F. Galbiati, F. Guzzi, A. I. Magee, G. Milligan, M. Parenti, *ibid.* **313**, 717 (1996).
9. P. T. Wilson and H. R. Bourne, *J. Biol. Chem.* **270**, 9667 (1995).
10. J. R. Hepler *et al.*, *ibid.* **271**, 496 (1996).
11. M. D. Edgerton, C. Chabert, A. Chollet, S. Arkinstall, *FEBS Lett.* **354**, 195 (1994); P. B. Wedegaertner, D. H. Chu, P. T. Wilson, M. J. Levis, H. R. Bourne, *J. Biol. Chem.* **268**, 25001 (1993).
12. J. Song and H. G. Dohlman, *Biochemistry* **35**, 14806 (1996).
13. H. K. W. Fong, K. K. Yoshimoto, P. Eversole-Cire, M. I. Simon, *Proc. Natl. Acad. Sci. U.S.A.* **85**, 3066 (1988); M. Matsuoka, H. Itoh, T. Kozasa, Y. Kaziro, *ibid.* **85**, 5384 (1988).
14. P. J. Casey, H. K. W. Fong, M. I. Simon, A. G. Gilman, *J. Biol. Chem.* **265**, 2383 (1990).
15. J. Wang, Y. Tu, J. Woodson, X. Song, E. M. Ross, *ibid.* **272**, 5732 (1997).
16. Sequence data indicate that the purified brain G_z GAP (*15*) is an RGS protein related to RET-RGS1 (*31*) and GAIP (*26*).
17. H. G. Dohlman and J. Thorner, *J. Biol. Chem.* **272**, 3871 (1997); M. R. Koelle, *Curr. Opin. Cell Biol.* **9**, 143 (1997).
18. J. A. Duncan and A. G. Gilman, *J. Biol. Chem.* **271**, 23594 (1996).
19. $G\alpha_z$ expressed in Sf9 cells is both myristoylated and palmitoylated (*2*), but palmitate is largely removed during purification. $G\alpha_z$ (4 μM) purified from Sf9 cells or myristoylated $G_{\alpha i1}$ from *E. coli* (*32*) was palmitoylated by incubation for 2 to 3 hours at 30°C with 50 μM Pal-CoA, either unlabeled or ^{3}H-labeled at 1000 cpm/pmol, in 50 mM NaHepes (pH 7.8), 2 mM EDTA, and 7.5 mM CHAPS detergent (*18*). [^{3}H]Palmitoylation was measured by liquid scintillation counting after precipitation with 10% trichloroacetic acid (*18*) or SDS–polyacrylamide gel electrophoresis (PAGE). The concentration of active $G\alpha_z$ was assayed according to the binding of 10 μM [^{35}S]GTP-γ-S (*15, 33*) except that the binding reaction mixture was incubated for 60 min in the presence of 25 mM $(NH_4)_2SO_4$, which increases the rate of nucleotide exchange on G-protein α subunits (*34*). Maximal observed binding of [^{35}S]GTP-γ-S was 65 to 70% of that predicted from assay of total protein.
20. Hydrolysis of $G\alpha_z$-bound [γ-^{32}P]GTP and G_z GAP activity were measured at 15°C as described (*15*). GAP activity is expressed either as the amount of bound GTP hydrolyzed above background at early times (quasi-linear time course) or as an apparent first-order rate constant (k_{app}). A unit of GAP activity is defined as an increment in k_{app} of 1 min^{-1} (*15*). Basal and stimulated hydrolysis of GTP bound to $G\alpha_{i1}$ was measured with a single-turnover assay (*15*) that included centrifugal gel filtration to remove unbound [γ-^{32}P]GTP and [^{32}P]Pi formed during the binding reaction.
21. To proteolyze $G\alpha_z$ near its NH_2-terminus, $G\alpha_z$ was first incubated with either 50 μM GTP-γ-S (30°C for 90 min) or 50 μM guanosine diphosphate (GDP), 30 μM $AlCl_3$, 10 mM NaF, and 10 mM $MgCl_2$ (15°C for 20 min) in 25 mM NaHepes (pH 7.5), 1 mM EDTA, 0.5 mM Mg^{2+}, 1 mM DTT, and 0.1% Triton X-100. The mixture was further incubated with trypsin (0.05 milligrams per milligram of $G\alpha_z$) at 30°C for 30 min. Phenylmethylsulfonylfluoride (1 mM) and tosyl-lysyl-chloromethylketone (0.2 mM) were added and digestion was checked by SDS-PAGE. Trypsin cleaved activated $G\alpha_z$ after Arg^{29}, according to automated Edman sequencing of the large tryptic fragment (*22*).
22. Y. Tu and J. Wang, unpublished data.
23. Both reversal of inhibition by DTT treatment and mock palmitoylation of $G\alpha_z$ without Pal-CoA were routine controls.
24. N. Watson, M. E. Linder, K. M. Druey, J. H. Kehrl, K. J. Blumer, *Nature* **383**, 172 (1996); J. R. Hepler, D. M. Berman, A. G. Gilman, T. Kozasa, *Proc. Natl. Acad. Sci. U.S.A.* **94**, 428 (1997).
25. D. M. Berman, T. M. Wilkie, A. G. Gilman, *Cell* **86**, 445 (1996).
26. L. De Vries, M. Mousli, A. Wurmser, M. G. Farquhar, *Proc. Natl. Acad. Sci. U.S.A.* **92**, 11916 (1995).
27. M. R. Koelle and H. R. Horvitz, *Cell* **84**, 115 (1996).
28. T. W. Hunt, T. A. Fields, P. J. Casey, E. G. Peralta, *Nature* **383**, 175 (1996).
29. Palmitoylation of $G\alpha_{i1}$ also blocked acceleration by RGS4 of M2 muscarinic cholinergic receptor-stimulated steady-state GTPase activity when assayed in reconstituted phospholipid vesicles as described (*15, 22*). The effect of palmitoylation does not therefore depend on interaction with detergent.
30. J. J. G. Tesmer, D. M. Berman, A. G. Gilman, S. R. Sprang, *Cell* **89**, 251 (1997). Direct and specific contact of RGS proteins with Cys^3 of Gα is not crucial, because mutation of this residue to Ala did not alter the responsiveness of $G\alpha_{i1}$ to RGS4 (*22*).
31. E. Faurobert and J. B. Hurley, *Proc. Natl. Acad. Sci. U.S.A.* **94**, 2945 (1997).
32. M. E. Linder *et al.*, *J. Biol. Chem.* **266**, 4654 (1991).
33. D. R. Brandt and E. M. Ross, *ibid.* **260**, 266 (1985).
34. K. M. Ferguson and T. Higashijima, *Methods Enzymol.* **195**, 188 (1991).
35. T. Kozasa and A. G. Gilman, *J. Biol. Chem.* **270**, 1734 (1995).

36. We thank A. Duncan for advice and [^{3}H]Pal-CoA, D. Berman for RGS4 protein and for GAIP cDNA, S. Popov for purified RGS10, P. Chidiac for advice, K. Chapman and J. Woodson for expert technical assistance, C. Slaughter and S. Afendis for peptide sequencing, and M. Cobb, S. Mukhopadhyay, and S. Sprang for comments on the manuscript. Supported by NIH grant GM30355, R. A. Welch Foundation grant I-0982, and a postdoctoral fellowship to J.W. from Cadus Pharmaceuticals Corp.

22 May 1997; accepted 30 September 1997

Areal Segregation of Face-Processing Neurons in Prefrontal Cortex

Séamas P. Ó Scalaidhe,* Fraser A. W. Wilson,† Patricia S. Goldman-Rakic

A central issue in cognitive neuroscience concerns the functional architecture of the prefrontal cortex and the degree to which it is organized by sensory domain. To examine this issue, multiple areas of the macaque monkey prefrontal cortex were mapped for selective responses to visual stimuli that are prototypical of the brain's object vision pathway—pictorial representations of faces. Prefrontal neurons not only selectively process information related to the identity of faces but, importantly, such neurons are localized to a remarkably restricted area. These findings suggest that the prefrontal cortex is functionally compartmentalized with respect to the nature of its inputs.

A major advance in understanding cortical organization has been the partitioning of large territories of cortex into regions on the basis of sensory modalities and submodalities (*1, 2*). This is particularly striking in the visual system, where processes related to central and peripheral vision can be traced from the retina to the highest levels of visual association cortex in the inferior temporal cortex (IT) and the posterior parietal cortex. The situation is less clear for prefrontal cortex. Because of its status as the archetypal association cortex, the functional architecture of prefrontal cortex has theoretical implications for the issue of whether association cortex has a modular functional organization like that of the sensory regions or is instead relatively undifferentiated. Evidence from the study of lesions (*3*),

Section of Neurobiology, Yale University Medical School, 333 Cedar Street, New Haven, CT 06510, USA.

*To whom correspondence should be addressed. E-mail: seamas@kafka.med.yale.edu

†Present address: ARL Division of Neural Systems, University of Arizona, Life Sciences North Building, Tuscon, AZ 85724, USA.

anatomical connections (*4*, *5*), and human imaging (6, but see *7*) indicates that the prefrontal cortex may also be partitioned on the basis of its sensory innervation. At the cellular level, electrophysiological studies have revealed spatially selective responses in the dorsolateral prefrontal cortex (8) and object-specific neural responses within the inferior prefrontal convexity of the macaque monkey (*9*, *10*). However, only a few studies have directly compared dorsal and ventral areas involved in spatial and object vision, respectively, and these studies have found either only quantitative differences (*11*) or no specialization of function at all (*12*). We reasoned that using an ecologically salient stimulus to map prefrontal cortex might reveal a degree of areal specialization that has not been evident in prior studies. Given that recognition of and interaction with one's conspecifics is critical to social behavior and relies heavily on the ability to discriminate between faces and facial expressions, neuronal responses to faces, as seen in inferior temporal cortex (*13*), provide such a probe. On the basis of extensive mapping, we now report that the prefrontal cortex contains a highly circumscribed region, the inferior prefrontal cortex, where neurons selectively process information contained in faces. Therefore, these results indicate that the ventral visual stream dedicated to stimulus identification in central vision (*1*) extends from visual cortex to the prefrontal cortex.

The results are based on 46 face-selective neurons from a sample recorded throughout the prefrontal cortex of three monkeys trained to maintain fixation while visual stimuli were presented (*14*). The analysis of neuronal activity to a wide variety of stimuli revealed that these neurons' responses were triggered by pictures of a face and gave little or no response to any pictures of nonface stimuli (Fig. 1A) (*15*). To determine whether the face-selective responses were determined by potentially confounding factors such as the emotional or motivational significance associated with faces or local visual features of certain faces, putative face-selective neurons were tested with a variety of additional stimuli. Neurons that showed responses to face stimuli were tested on an array of additional stimuli with strong motivational or emotional significance to the monkeys such as monkey chow, fruit, leather handling gloves, snakes, insects, and the like. There was no sign that motivational or emotional significance of the stimuli was a determining factor in the responses to faces. Indeed, the only significant difference due to stimulus class (faces, objects, colored rectangles, peripherally presented spots of light, common "laboratory" stimuli such as oriented lines, emotionally significant stimuli, and motivationally significant stimuli) in the responses of face-selective neurons was between faces and other stimuli ($P < 0.00013$; Tukey Honestly Significant Difference test). Face-selective responses were also not determined by local features within the face. Instead, the neurons appeared to respond to the face as an identifiable object, because their response was greatly diminished or eliminated when the same face was scrambled to preserve elements such as internal texture, color, and local contours but lacked the immediate impression of a face to a human observer (Fig. 1B; two-tailed t test for paired observations, $P = 0.00002$). To further determine that the selective responses to faces were not merely the result of local features idiosyncratic to certain face stimuli, six face-selective neurons were tested with the same sets of 10 stimuli inverted, converted to black and white, and decreased in size. As is the case in IT (*16*), stimulus identity was strongly correlated with response magnitude across manipulations (Pearson $r = -0.877$, $P < 10^{-9}$). In contrast, manipulation of stimulus orientation, size, or color versus black and white did not significantly affect response magnitude ($r = 0.132$, $P = 0.418$).

Because foveation is a critical aspect of stimulus identification, it would be expected that neurons processing such information would exhibit their best responses to foveal stimulation, and, indeed, this was the case when 11 face-selective neurons were tested with faces at nine locations: foveally and at eight locations 13° from the fixation point

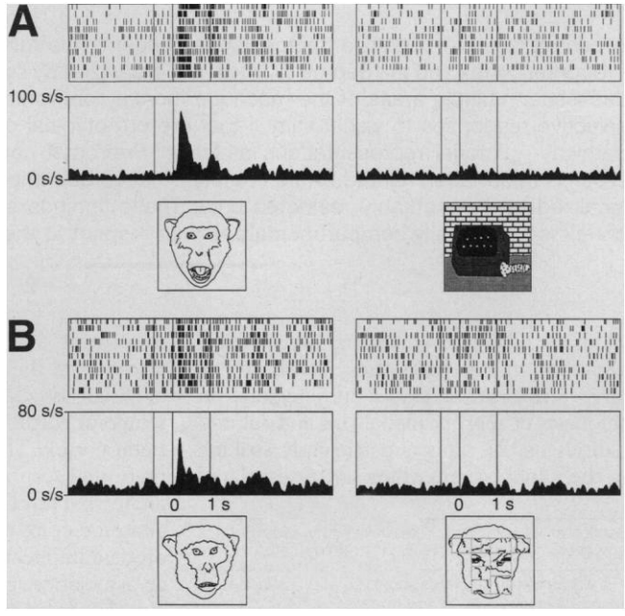

Fig. 1. (**A**) Trial by trial rasters and averaged spike density functions (SDFs) of one face-selective cell to the most effective face and the most effective nonface stimulus with which it was tested. Each raster tick denotes one extracellularly recorded action potential, and the SDFs are averaged neural activity convolved with a Gaussian function (SD = 30 ms). For all rasters and SDFs, the first vertical line denotes the animal's foveation of the fixation point, the second vertical line indicates stimulus onset, and the third vertical line indicates stimulus offset. The duration of the stimulus was 1 s. The actual stimuli were color images presented on a computer monitor (*14*). The ordinate represents the neural response in spikes per second (s/s). (**B**) The mean response of the same face-selective neuron to another face and to this face scrambled. Conventions are as in (A).

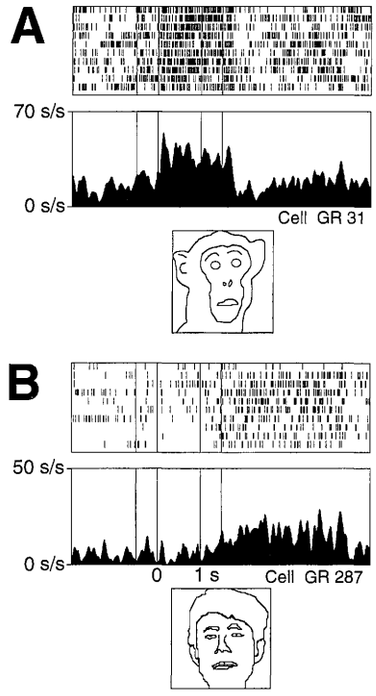

Fig. 2. (**A**) A neuron with a visual response which persists after the offset of the visual stimulus. Conventions are as in Fig. 1, with a fourth vertical line indicating the offset of the fixation point and delivery of reward. (**B**) A different neuron, with face-selective post-stimulus activity in the absence of a visual response. Conventions are as in (A). There was a strong and lasting post-stimulus response to the face and not to any of the other stimuli. This activity continued throughout the intertrial interval and was not related to eye movements or to any other observable behavior that followed the face stimulus during the posttrial period.

(12.7 versus 5.0 spikes per second over baseline; $P = 0.00016$, two-tailed t test for unpaired observations). Typically, there was a maximal response to foveal stimulation and weaker responses to a subset of the extrafoveal stimuli. The foveal emphasis and relatively large receptive fields of face-selective neurons are similar to neurons in IT cortex (*13*).

An interesting feature of face-selective responses was their marked tendency to either continue or begin firing after stimulus offset. We observed two types of persistent responses. First, "onset" face-selective visual responses that began with stimulus onset and persisted from 200 to 1500 ms after offset of the visual stimulus were observed for 15/18 of the face-selective neurons with tonic responses (Fig. 2A) (*17*). Most remarkably, in six face-selective neurons, we observed a second type of persistent face-selective activity: "offset" responses (Fig. 2B) that began only after stimulus offset and lasted for up to 2600 ms (until the next trial began). The firing of these neurons was not related to eye movements or to any other observable behavior particular to the offset of the face stimuli. These responses, indistinguishable from stimulus-selective delay activity seen in memory tasks, were observed both in two monkeys that had been trained on memory tasks and in a monkey that viewed visual stimuli while fixating but was never trained on a memory task. Thus, the capacity for face-selective persistent firing and delay-period activity does not depend on intention to make a response, but appears to reflect an intrinsic property of the neurons' responses to visual stimuli.

A full characterization of the face-specific neurons examined here involves description of their localization within the prefrontal cortex. A deliberate attempt was made to record from as wide an area of the dorsolateral and lateral orbital regions of the prefrontal cortex as possible to address the difficult issue of whether information processing is segregated in prefrontal cortex as it is in the visual system (*18*). A detailed reconstruction of the sites from which face-selective neurons were recorded revealed (Fig. 3) (*19*) that more than 95% (44/46) were located in the regions of the prefrontal cortex that receive input from the temporal lobe visual areas (the other two neurons were located in the posterior bank of the dorsal ramus of the arcuate sulcus). All of the neurons with face-selective visual responses were located in the inferior convexity ($n = 37$), the lateral orbital cortex ($n = 4$), and the arcuate sulcus ($n = 3$). In contrast, not one of 480 units tested in the principal sulcus or of the 180 recorded in the superior prefrontal convexity was selective for faces. Similarly, of the 300 neurons tested with faces in a memory task (*10*), all of the neurons with selective responses to faces in the delay period were located in the IT-recipient prefrontal cortex (4/6 of these neurons also had face-selective visual responses). None of the cells in the principal sulcus (0/56) or superior prefrontal convexity (0/81) responded selectively in the delay period to a picture of a face. Finally, to determine the connections of this region, we injected two monkeys with wheat germ agglutinin–horseradish peroxidase or fluorescent dyes at the termination of cellular recordings. The physiologically defined areas received input from the ventral bank of the superior temporal sulcus and adjacent cortex on the inferior temporal gyrus—regions from which face-selective neurons have been recorded in previous studies (*16*, *20*). The anatomical connections [see also (*4*)] account for why the neurons of the inferior prefrontal cortex are more similar in their visual selectivity to those in the temporal lobe than they are to those of the dorsolateral prefrontal cortex.

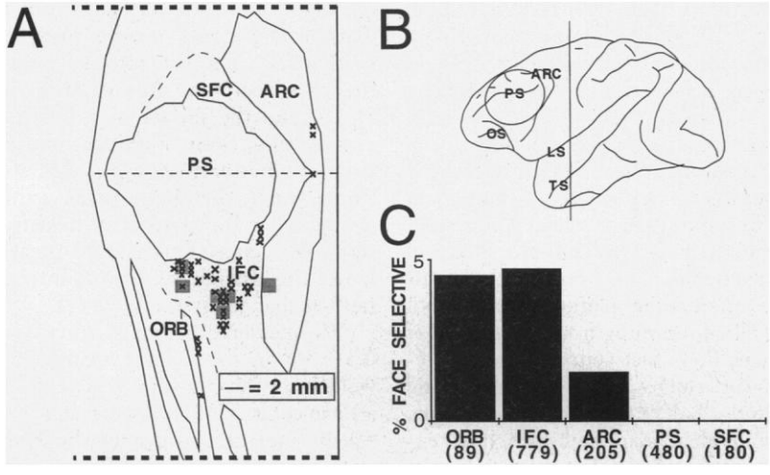

Fig. 3. The locations of face-selective neurons. (**A**) The location of neurons with face-selective visual responses are indicated on a flattened representation of the prefrontal cortex by x's, and the locations of neurons with delay activity selective for faces are indicated by shaded squares (four neurons had both visual and delay responses). The boundary between the IFC and ORB is indicated by a dashed line, and the boundary between the IFC and SFC is indicated by the dashed line bisecting the PS. The anterior and dorsal extent of the recording area in the SFC is indicated by a dashed line. (**B**) The typical location of the recording chamber is shown on the lateral view of the brain as a circle around the PS. (**C**) The percentage of neurons [out of all neurons sampled, see (*18*)] with face-selective visual responses in each prefrontal region. Abbreviations are as follows: IFC, inferior convexity; ARC, arcuate sulcus; PS, principle sulcus; OS, orbital sulcus; LS, lateral sulcus; TS, inferior temporal sulcus; ORB, lateral orbitofrontal cortex; SFC, superior frontal convexity (dorsal to PS and anterior to ARC).

REFERENCE AND NOTES

1. L. G. Ungerleider and M. Mishkin, in *Analysis of Visual Behavior*, D. J. Ingle, M. A. Goodale, R. J. W. Maunsfield, Eds. (Massachusetts Institute of Technology Press, Cambridge, MA, 1982), pp 549–586; A. Morel and J. Bullier, *Visual Neurosci.* **4**, 555 (1990); D. J. Felleman and D. C. Van Essen, *Cereb. Cortex* **1**, 1 (1991).
2. M. M. Merzenich and J. F. Brugge, *Brain Res.* **50**, 275 (1973); C. J. Robinson and H. Burton, *J. Comp. Neurol.* **192**, 69 (1980).
3. C. G. Gross and L. Weiskrantz, *Exp. Neurol.* **5**, 453 (1962); P. S. Goldman and H. E. Rosvold, *ibid.* **27**, 291 (1970); R. Passingham, *Brain Res.* **92**, 89 (1975); M. Mishkin and F. J. Manning, *ibid.* **143**, 313 (1978).
4. S. Jacobson and J. Q. Trojanowski, *Brain Res.* **132**, 209 (1977); K. Kawamura and J. Naito, *Neurosci. Res.* **1**, 89 (1984); H. Barbas, *J. Comp. Neurol.* **276**, 313 (1988); H. R. Rodman, *Cereb. Cortex* **5**, 484 (1994); M. J. Webster, J. Bachevalier, L. G. Ungerleider, *ibid.*, p. 470; J. F. Bates, F. A. W. Wilson, S. P. Ó Scalaidhe, P. S. Goldman-Rakic, *Soc. Neurosci. Abstr.* **21**, 1054 (1995); J. Bullier, J. D. Schall, A. Morel, *Behav. Brain Res.* **76**, 89 (1996).
5. H. Barbas and M.-M. Mesulam, *Neuroscience* **15**, 619 (1985); C. Cavada and P. S. Goldman-Rakic, *J. Comp. Neurol.* **287**, 422 (1989); R. A. Andersen, C. Asanuma, G. Essick, R. M. Siegel, *ibid.* **296**, 65 (1990).
6. S. M. Courtney, L. G. Ungerleider, K. Keil, J. V. Haxby, *Cereb. Cortex* **6**, 1047 (1996); G. McCarthy *et al.*, *ibid.*, p. 600.
7. A. M. Owen, *Trends Cogn. Neurosci.* **4**, 123 (1997).
8. K. Kubota and H. Niki, *J. Neurophysiol.* **34**, 337 (1971); J. M. Fuster, *ibid.* **36**, 61 (1973); H. Suzuki and M. Azuma, *Exp. Brain Res.* **53**, 47 (1983); R. A. Boch and M. E. Goldberg, *J. Neurophysiol.* **61**, 1064 (1989); S. Funahashi, C. J. Bruce, P. S. Goldman-Rakic, *ibid.*, p. 331.
9. I. N. Pigarev, G. Rizzolatti, C. Scandolara, *Neurosci. Lett.* **12**, 207 (1979).
10. F. A. W. Wilson, S. P. Ó Scalaidhe, P. S. Goldman-Rakic, *Science* **260**, 1955 (1993).
11. V. P. Ferrera, K. K. Rudolph, J. H. R. Maunsell, *J. Neurosci.* **14**, 6171 (1994); A. B. Sereno and J. H. R. Maunsell, *Soc. Neurosci. Abstr.* **21**, 282 (1995); A. B. Sereno, C. J. McAdams, J. H. R. Maunsell, *ibid.* **23**, 302 (1997).
12. S. C. Rao, G. Rainer, E. K. Miller, *Science* **276**, 821 (1997).
13. C. G. Gross, C. E. Rocha-Miranda, D. B. Bender, *J. Neurophysiol.* **35**, 96 (1972); C. G. Gross, D. B. Bender, M. Mishkin, *Brain Res.* **131**, 227 (1977); R. Desimone and C. G. Gross, *ibid.* **178**, 363 (1979); R. Desimone, T. D. Albright, C. G. Gross, C. Bruce, *J. Neurosci.* **4**, 2051 (1984); H. R. Rodman, S. P. Ó

Scalaidhe, C. G. Gross, *J. Neurophysiol.* **70**, 1115 (1993).
14. Monkeys were trained by successive approximation to fixate within 2.0° of the fixation point. If the animal's eye position left the fixation window, the fixation light extinguished, no reward was delivered, and a 1 s time-out was imposed in addition to the intertrial interval. A trial consisted of: fixation of a centrally presented fixation point for 0.5 s, 1.0 s of visual stimulus presentation, followed by an additional 0.5 s of fixation. No behavioral response other than visual fixation was required, and stimuli were presented in a randomized order. Every neuron was tested on one or more basic sets of color stimuli presented on a computer monitor including faces, objects, and colored rectangles. Stimuli typically subtended 8° to 10° of visual angle and were presented on a monitor with 640 pixel by 400 pixel resolution and 16-bit color. In two of three monkeys, when neurons appeared to show selectivity for faces, they were then tested exhaustively with additional stimuli to assess the basis for an apparent selective response to a face stimulus.
15. The mean firing rate was calculated for five time intervals for the task: 1 s during the pretrial period preceding the onset of the fixation point, 400 ms starting 100 ms after visual fixation, 200 ms beginning 100 ms after presentation of the visual stimulus, 900 ms from 100 ms after onset of the visual stimulus, and 2000 ms starting 100 ms after offset of the visual stimulus. An analysis of variance (ANOVA) was then performed using stimulus as a factor and firing rate in the time windows as a factor with repeated measures. The ANOVA yielded P values for the effects of time period, stimulus, and interaction between stimulus and time period. Only neurons with a significant main effect of stimulus or a significant interaction between stimulus and time window and a significant one-way ANOVA for one of the cue periods or the postcue period at a level of $P < 0.05$ were considered selectively responsive. Using the criteria of Perret and colleagues (*20*), cells that met the ANOVA criteria and had a response magnitude to the best face stimulus that was more than twice as strong as the best response to a nonface stimulus were considered to be face-selective.
16. E. L. Schwartz, R. Desimone, T. D. Albright, C. G. Gross, *Proc. Natl. Acad. Sci. U.S.A.* **80**, 5776 (1983); E. T. Rolls and G. C. Baylis, *Exp. Brain Res.* **65**, 38 (1986); G. Sáry, R. Vogels, G. A. Orban, *Science* **260**, 995 (1993).
17. Offset of response was determined by when the response returned to below (or above) a 95% confidence interval based on pretrial firing for at least 100 ms [J. M. MacPherson and J. W. Aldridge, *Brain Res.* **175**, 183 (1979)].
18. To enable an unbiased sample of neurons, and therefore meaningful intraregional comparisons, neurons were not preselected for visual responsiveness, visual selectivity, or any other form of task-related activity.
19. Flattened representations of the prefrontal cortex were constructed with methods similar to D. C. Van Essen and J. H. R. Maunsell [*J. Comp. Neurol.* **191**, 255 (1980)] as modified by H. Barbas (*4*). The location of each face-selective neuron was drawn on a tracing of the appropriate section through the monkey's brain, these sections were compared to sections of a cortical atlas, and the neurons' location was transferred to the atlas. Then the cortical atlas with the locations of the cells was flattened along the midpoint between white matter and the pial surface.
20. D. I. Perret, E. T. Rolls, W. Caan, *Exp. Brain Res.* **47**, 329 (1982); G. C. Baylis, E. T. Rolls, C. M. Leonard, *J. Neurosci.* **7**, 330 (1987).
21. Experiments were conducted in accordance with the Yale University Animal Care Committee. Supported by National Institute of Mental Health grants MH44866 and MH38546 to P.S.G.-R. and by McDonnell Foundation fellowship JSMF 91-47 to S.P.Ó.S. We thank M. Chafee, K. McEvoy, L. Romanski, and N. Vnek for comments on preliminary drafts of the manuscript.

23 July 1997; accepted 3 October 1997

Thermoregulation in the Mouths of Feeding Gray Whales

John E. Heyning and James G. Mead

Vascular structures for heat conservation in the tongue of the gray whale (*Eschrichtius robustus*) are reported here. Numerous individual countercurrent heat exchangers are found throughout the massive tongue. These converge at the base of the tongue to form a bilateral pair of retia. Temperature measurements from the oral cavity of a live gray whale indicate that more heat may be lost through the blubber layer over the body than through the tongue, despite the fact that the tongue is far more vascularized and has much less insulation. These heat exchangers substantially reduce heat loss when these whales feed in cold waters.

Because of the high thermal conductivity of water, the oceans and seas are energetically challenging environments for endotherms. Countercurrent heat exchangers in the vascular system of whales assist in the regulation of body temperature (*1*): those within the fins and flukes (*2*) function to conserve core body temperature, whereas those associated with the reproductive tracts (*3*) serve to prevent hyperthermia in these heat-sensitive organs. The mouths of baleen whales (suborder Mysticeti) are relatively large, in order to accommodate the filtering surface composed of baleen, and the oral cavity of baleen whales is a major site for heat loss during feeding. To date, there have been no measurements to quantify this loss (*4*), nor have any structures been identified that would serve to reduce it.

In each of two young gray whale calves dissected (*5*) (LACM 88981, 3.98 m long; and LACM 92044, 5.25 m long), we found numerous individual countercurrent heat exchangers spaced throughout the tongue (Fig. 1A). These periarterial venous retia (*6*) consist of a single central artery encircled by a sheath of surrounding veins and are about 0.5 cm in diameter, making them similar in size to the individual countercurrent heat exchangers within the flukes of the same animals. The groups of blood vessels are oriented in planes, so that cool venous blood returning from the surface of the tongue flows first ventrally then posteriorly toward the back of the tongue. Along the posterior half of the base of the tongue, these individual countercurrent heat exchangers converge to form a bilateral pair of large vascular retia (Fig. 1B), each composed of over 50 such heat exchangers oriented adjacent and parallel. We term each vascular bundle a lingual rete. In the 5.25-m calf, each of these lingual retia was about 13 by 2 cm in cross-section and approximately 55 cm long. The lingual retia form one of the largest countercurrent heat exchangers described in any endotherm (*2*, *3*). At the base of the tongue, these heat-exchanger retia sweep dorsally and separate into numerous individual arteries and veins that connect to the external carotid artery and jugular vein, respectively. The countercurrent vascular retia are situated in the fascial plane located between the tongue muscles (styloglossus, hyoglossus, and intrinsic tongue muscles) and the more superficial gular muscles (geniohyoideus and myohyoideus). This vascular complex is derived from the lingual arteries and veins.

The distinct lingual artery is short, bifurcating into numerous arteries about 3 cm distal to the external carotid artery. This proliferation of arteries just proximal to the lingual rete functionally increases the cross-sectional area of this vascular system and the surface area of the blood vessel walls. Both of these structural attributes function to slow blood flow in any single vessel, thereby increasing the time available for the transfer of heat from arteries to veins. This should greatly enhance the efficiency of the countercurrent heat-exchanger system.

We measured a lingual surface area of 0.325 m^2 in the 5.25-m specimen, which yields an estimated surface area of 2 m^2 for a 12-m adult. This represents approximately 5% of the surface area of the body (*7*), excluding the extremities. Because a mobile and dexterous tongue is needed to control water flow over the baleen, the tongue could not properly function if it were cloaked with a thick, semirigid adipose layer similar to the blubber encasing the body. However, the outer surface of the tongue is invested with a diffuse layer of fatty tissue about 2 cm thick.

Skin surface temperature relative to ambient temperature is a good indicator of

J. E. Heyning, Section of Vertebrates, Natural History Museum of Los Angeles County, 900 Exposition Boulevard, Los Angeles, CA 90007, USA. E-mail: heyning@bcf.usc.edu
J. G. Mead, Division of Mammals, National Museum of Natural History, Washington, DC 20560, USA. E-mail: mead.james@nmnh.si.edu